Separation Science and Technology
Publication details, including instructions for authors and subscription information:
http://www.informaworld.com/smpp/title~content=t713708471

Membrane Sieving of a Continuous Polydisperse Mixture through Distributed Pores

Benjamin J. McCoy[a]
[a] DEPARTMENT OF CHEMICAL ENGINEERING AND MATERIALS SCIENCE, UNIVERSITY OF CALIFORNIA DAVIS, CALIFORNIA

To cite this Article McCoy, Benjamin J.(1995) 'Membrane Sieving of a Continuous Polydisperse Mixture through Distributed Pores', Separation Science and Technology, 30: 4, 487 — 507
To link to this Article: DOI: 10.1080/01496399508225606
URL: http://dx.doi.org/10.1080/01496399508225606

SEPARATION SCIENCE AND TECHNOLOGY, **30**(4), pp. 487–507, 1995

Membrane Sieving of a Continuous Polydisperse Mixture through Distributed Pores

BENJAMIN J. McCOY
DEPARTMENT OF CHEMICAL ENGINEERING AND MATERIALS SCIENCE
UNIVERSITY OF CALIFORNIA
DAVIS, CALIFORNIA 95616
TELEPHONE: (916) 752-6923; FAX: (916) 752-1031; bjmccoy@ucdavis.edu

ABSTRACT

A mathematical theory is presented to describe membrane sieving based on the relative sizes of pores and solutes. A polydisperse liquid mixture with a continuous distribution of solute radii undergoes hindered transport through distributed membrane pores. The hydrodynamic theory for rigid spheres in cylindrical pores provides expressions for the hindered diffusive and convective fluxes. Continuous and discrete (including fractal) distributions of pore sizes are considered. For a steady-state ultrafiltration process with a well-mixed upstream concentration distribution, the theory predicts how much the downstream concentration distribution shifts toward smaller solutes as larger solutes are hindered or rejected by the membrane. Sieving coefficients, which are related to permeation rates that depend on relative pore and solute sizes, are presented for gamma distributions of solute radii and for continuous and discrete pore-radii distributions.

Key Words. Theory; Ultrafiltration; Fractal pore-size distribution; Hindered diffusion; Polydisperse mixture

INTRODUCTION

Membrane separations of liquid mixtures can occur by an ultrafiltration seiving process in which smaller solutes pass through the pores and larger solutes are retarded or totally rejected (1–3). Despite the practical importance of such partially-retentive membranes (4), relatively little work has

been reported for solutes of many different sizes in distributed pores. In their discussion of dextran transport through ultrafiltration membranes, Mochizuki and Zydney (2) reviewed the experimental investigations of such polydisperse solutions. In the absence of surface forces that cause adsorption, the separation is due to steric effects in the membrane pores. Solutes of all sizes are hindered in their convective or diffusive passage through the membrane by interaction with the pore walls. These hydrodynamic interactions can be mathematically characterized for certain cases, including rigid spheres in cylindrical pores and in rectangular slits (5, 6).

The current investigation proposes and evaluates a pore-transport model for ultrafiltration separations of a continuous liquid mixture whose distribution of solute sizes is a continuous function. Continuous-mixture theories have provided a useful route for understanding thermodynamics and chemical kinetics in multicomponent mixtures (7–11), but have not been applied extensively to problems of mass transfer and separation. The present objective is to show how a model can be developed for transport of continuous mixtures in distributed pores and to examine the consequences of the model. The distribution of the solute radii is taken to be a gamma distribution, a versatile function for describing continuous frequency distributions (9, 10).

The membrane consists of cylindrical pores, perpendicular to the membrane surface, whose sizes are represented by a pore-size distribution. The mixture has so many chemical species that it is described by a continuous function of solute radius, which itself is a continuous independent variable. The convection and diffusion of the solutes, assumed to be neutral rigid spheres, through the cylindrical pores are hindered by steric interactions with the pore walls, thus reducing the flux. Only solutes smaller than the pore diameter are allowed to be transported through the membrane. The effect of this pore cutoff diameter is enhanced by hindered transport to afford a basis for separation. The theory of hindered transport in liquid-filled pores has been developed for several geometries, including single spheres in a cylindrical pore (5). Using the approximation that each such sphere is positioned on the centerline, Bungay and Brenner (6) derived an expression for diffusive and convective flux for all solute diameters smaller than the pore diameter. The discussion here is restricted to membrane separations in the absence of external mass transfer limitations. Opong and Zydney (3) and Mochizuki and Zydney (2) explained how to account for such concentration polarization effects. Dharmappa et al. (12) discussed how solute polydispersivity affects membrane fouling.

Both continuous and discrete pore-size distributions are treated in the present mathematical model of membrane sieving. Rectangular distributions of pore radii illustrate how continuous functions enter into the model

formulation and influence the results. A discrete pore-size distribution is introduced by a fractal approach based on the concept of the Sierpinski carpet (13) and constructed by an iterative, deterministic procedure. The pore distribution allows for the number of pores and their size to be represented by a fractional power, i.e., the fractal dimension. The fractal reduces to the Sierpinski carpet membrane when appropriate values of three parameters are chosen. Such fractals were proposed by Adler (14) but not applied to diffusion of mixtures. Sernetz et al. (15) recognized the importance of the diffusion of a mixture of different-sized molecules in fractal porous media for chromatographic separations.

The current paper is arranged so that flux through a single pore is discussed in terms of the well-mixed upstream and downstream solute distributions, $c_0(x)$ and $c_f(x)$. The summation of fluxes through *all* pores provides expressions for the total permeation rate of solutes through the membrane. This allows the definition of a solute-dependent sieving coefficient, $s(x)$, that can be utilized to calculate the downstream distribution of solute sizes from the upstream distribution. The overall, or lumped, membrane sieving coefficient, S, can be found by integrations over x. Illustrative calculations are discussed for gamma distributions of solute radii and for continuous (rectangular and gamma) and discrete (fractal) pore-size distributions. With the given concepts and definitions, however, the approach can be applied using *any* functional forms for the distributions.

HINDERED TRANSPORT

A porous membrane is fixed between two large-volume, well-stirred bulk liquid mixtures. The liquids consist of a solvent containing continuous polydisperse mixtures with the solute radius as the independent variable. For such mixtures the concentration of solutes with radii in the range $(x, x + dx)$ is $c(x)dx$. The total, or lumped, concentration is

$$C = \int_0^\infty c(x)\, dx \tag{1}$$

A discrete number of solute species of size x_i and concentration C_i can be represented in terms of Dirac delta functions by the summation over the species:

$$c(x) = \sum C_i \delta(x - x_i) \tag{2}$$

The steady-state solute flux, $J(x, r_j)$, of a single solute through a single

pore of radius r_j is given by (1, 3, 5)

$$J = K_c v_j c - K_d D_b \, dc/dz \tag{3}$$

where $c(x, r_j, z)$ is the radially-averaged solute concentration distribution in the pore, v_j is the radially-averaged solution velocity, $D_b(x)$ is the bulk solution Brownian-motion diffusivity, and K_c and K_d are the hindrance factors for convective and diffusive transport, respectively. For laminar flow in a cylindrical pore of radius r_j, the velocity is given in terms of the bulk viscosity μ and the pressure difference Δp across the membrane of thickness L,

$$v_j = (r_j^2/8\mu)\Delta p/L \tag{4}$$

The hindrance factors, according to the Bungay and Brenner (6) theory, are expressed in terms of the partition coefficient (16, 17):

$$\Phi = (1 - x/r_j)^2, \qquad \text{for } x < r_j \tag{5}$$

$$\Phi = 0, \qquad \text{for } x \geq r_j$$

which accounts for exclusion of the spherical solute from an annular region of the pore, or from the pore itself if the sphere is larger than the pore. For diffusion and convection, respectively, the factors are functions of x and r_j,

$$K_d = 6\pi/K_t \qquad \text{and} \qquad K_c = (2 - \Phi)K_s/2K_t \tag{6}$$

where

$$(K_t, K_s) = (9/4)\sqrt{2\pi^2}(1 - x/r_j)^{-5/2}\,[1 + \textstyle\sum_1^2 (a_n, b_n)(1 - x/r_j)^n] + \textstyle\sum_0^4 a_{n+3}, b_{n+3})(x/r_j)^n \tag{7}$$

and the values for a_n and b_n are given in the Nomenclature Section. The hindrance factors apply to dilute suspensions of spheres, as solute–solute interactions are neglected.

The boundary conditions for the differential Eq. (3) for $c(x, r_j, z)$ in terms of the well-stirred bulk concentration distribution upstream, $c_0(x)$, and downstream, $c_f(x)$, are

$$c(x, r_j, z = 0) = \Phi c_0(x) \tag{8}$$

and

$$c(x, r_j, z = L) = \Phi c_f(x) \tag{9}$$

where the partition coefficient, Φ, accounts for exclusion of the spherical solute from an annular region of the pore, and ensures that $c(x, r_j, z)$ is

zero if $x \geq r_j$ due to the complete exclusion of a sphere from the pore. Thus the partition coefficient, defined in Eq. (5), enforces the cutoff requirement for each pore and thus for the membrane as a whole.

The solution to the differential Eq. (3) for the single pore is (1, 3)

$$J(x, r_j) = \Phi K_c v_j c_0 (1 - e_j{}^{P} c_f/c_0)/(1 - e_j^{-P}) \tag{10}$$

where the Peclet number for the solute of radius x and pore of radius r_j is defined as

$$P_j(x) = K_c v_j L / K_d D_b \tag{11}$$

Since the expression for J contains the multiplicative factor Φ, the flux vanishes for $x \geq r_j$.

The solute flux for each pore is multiplied by its cross-sectional area to determine the permeation rate (moles/time) through the pore, i.e., $\pi r_j^2 J(x, r_j)$. For discrete pore sizes, the permeation rate of solutes of radius x is the sum over all pore sizes,

$$N(x) = \sum n_j \pi r_j^2 J(x, r_j) \tag{12}$$

where n_j is the number of pores of radius r_j. The total volumetric flow rate for dilute solutions is

$$Q = \sum n_j \pi r_j^2 v_j \tag{13}$$

The downstream, well-stirred distribution of solute, $c_f(x)$, is the solute permeation rate, $N(x)$, divided by the volumetric flow rate, Q:

$$c_f(x) = N(x)/Q \tag{14}$$

Since $c_f(x)$ and $c_0(x)$ are independent of the pore size, we can combine and rearrange algebraically Eqs. (10) and (12)–(14) to obtain

$$s(x) = c_f(x)/c_0(x) = \sum [q_j F_j] / \sum q_j [1 + F_j \exp(-P_j)] \tag{15}$$

where

$$q_j = n_j \pi r_j^2 v_j \tag{16}$$

and

$$F_j = \Phi K_c / (1 - \exp(-P_j)) \tag{17}$$

In calculations of the ratio $s(x)$, constant factors such as $(1/8\mu)\Delta p/L$ in the expression for v_j and the normalization factor for the pore-size distribution will cancel. Within each summation the partition coefficient, Φ, serves to exclude solutes that are larger than a pore. This constitutes the pore cutoff property for *each* size pore. The sieving coefficient, $s(x)$, will

in general have a maximum asymptotic value less than unity because solutes larger than r_j are excluded from a pore of radius r_j. If the largest pores are much larger than the solutes, then $s(x)$ will approach unity. Defective membranes with a few large pores thus accomplish poor separation.

The calculation of $s(x)$ is closely related to the computation used by Mochizuki and Zydney (1) to calculate the sieving coefficient for a monodisperse solution. With the explicit representation of $s(x)$ in Eq. (15), however, an iterative solution method is unnecessary. The sieving coefficient $s(x)$ is independent of the *form* of the solute distributions, $c_0(x)$ and $c_f(x)$. If a value of $s(x)$ is known, then the downstream distribution can obviously be determined as

$$c_f(x) = s(x)c_0(x) \tag{18}$$

which shows the benefit of knowing $s(x)$. For a monodisperse pore-size distribution ($j = 1$), the sieving coefficient reduces to

$$s(x) = \Phi K_c e_1^P/[e_1^P - 1 + \Phi K_c] \tag{19}$$

consistent with the condition that $J = v_1 c_f$ (a special case of Eq. 14), which was discussed by Mochizuki and Zydney (1).

The overall sieving coefficient is defined as the ratio of the lumped downstream to the lumped upstream concentration,

$$S = C_f/C_0 = \int_0^\infty dx\, s(x)c_0(x)/\int_0^\infty dx\, c_0(x) \tag{20}$$

Because of the presence of Φ in $s(x)$, S will manifest a membrane cutoff since solutes larger than the largest pore will be excluded. The membrane sieving coefficient S depends on the form of $c_0(x)$, while $s(x)$ does not. For monodisperse solute distributions, $s = S$.

The function selected to represent the *upstream* continuous-mixture distribution of solute sizes is a gamma distribution, or Pearson Type III function (18), expressed in terms of $y = (x - x_0)/\beta$,

$$c_0(x) = (C_0/\beta\Gamma(\alpha))y^{\alpha-1}\exp(-y), \qquad \text{for } x \geq x_0$$

and

$$c_0(x) = 0, \qquad \text{for } x < x_0 \tag{21}$$

The zero moment with respect to x is C_0, the first moment is $x_{avg} = x_0 + \alpha\beta$, and the variance is $\alpha\beta^2$. The maximum of $c_0(x)$ is located at $x = x_0 + (\alpha - 1)\beta$. Depending on the magnitude of α, the gamma distribution can represent a spectrum of shapes between exponential ($\alpha = 1$) and gaussian ($\alpha \gg 1$). If $\alpha = 1$, $\beta = 1$, and $x_0 = 0$, Eq. (21) is the Poisson

distribution; if $\alpha = 1$ and $y \ll 1$, Eq. (21) is approximated by a rectangular distribution. To avoid the exclusion effect of solutes larger than the maximum pore size r_m, which would yield asymptotic values of S and $s(x > r_m)$ less than unity, in the computations to follow we truncate the gamma distribution so that $c_0(x > r_m) = 0$.

Figure 1 shows the gamma distribution for $\alpha = 2$, $C_0 = 1$, and $\beta = 5$ and 15. Increasing β when α is constant obviously broadens the distribution. To plot results as dimensionless variables, a length scale is needed. According to the gamma distribution, Eq. (21), the continuous mixture has a minimum solute radius, x_0. This parameter is a convenient basis for scaling x and r as x/x_o and r/x_o, although any length parameter would suffice. The Peclet number can be written as

$$P_j(x) = (r_j/x_0)^2 (K_c/K_d)T_0 \tag{22}$$

where

$$T_0 = \Delta p x_0^2/8\mu D_b \tag{23}$$

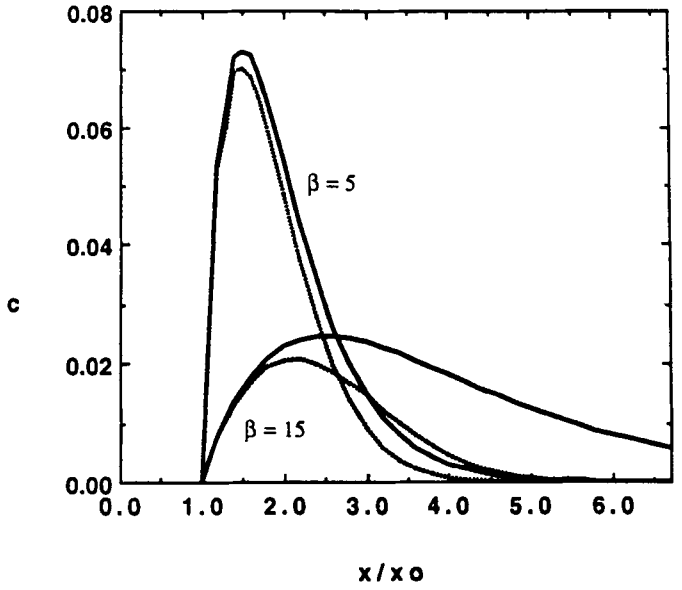

FIG. 1 Gamma distributions, $c_0(x)$, of upstream solute radii for $s = 2$, $C_0 = 1$, $\beta = 5$ and 15 (solid line). Downstream of the membrane with $T_0 = 0.001$ and a fractal pore distribution ($h = 2$, $s = 1.5$, $\Omega = \pi$, $a = 10x_0$), the distribution $c_f(x)$ (dotted line) demonstrates that solutes larger than $x_m/x_0 = 6.67$ are prevented from passing through pores and transport of smaller solutes is hindered.

is a dimensionless parameter that depends on the transmembrane pressure and therefore can be controlled experimentally (2).

The distributions for $c_f(x)$, plotted for a discrete fractal pore-size distribution at $T_0 = 0.001$ in Fig. 1, demonstrate the separation of larger solutes by pore cutoff and hindered transport. The downstream distribution, $c_f(x)$, is a gamma function only in special cases, e.g., when $s(x)$ is constant with x.

CONTINUOUS PORE-SIZE DISTRIBUTIONS

If the pore sizes are distributed continuously, then the summations in the above equations are replaced by integrals over a pore-size distribution, $n(r)$, where the number of pores in the size range $(r, r + dr)$ is $n(r)\,dr$. Then instead of the summation in Eq. (12), the permeation rate of solutes of radius x is the integral over $n(r)$,

$$N(x) = \int_0^\infty dr\, n(r)\pi r^2 J(x, r) \tag{24}$$

and likewise for Q in Eq. (13). The algebraic manipulations needed to write the sieving coefficient are the same as for the discrete case; one obtains

$$s(x) = c_f(x)/c_0(x) \tag{25}$$

$$= \left[\int_0^\infty dr\, q(r)F(r)\right] \Big/ \left[\int_0^\infty dr\, q(r)[1 + F(r)e^{-P}\right]$$

where, for example,

$$q(r) = n(r)\pi r^2 v \tag{26}$$

and we have simply dropped the subscript j on the continuous variables r, q, v, P, and F. The ratio that defines $s(x)$ ensures that the normalization constant of the pore-size distribution has no influence on $s(x)$. The expression for the membrane sieving coefficient for continuous pore-size distributions is the same as discrete distributions, Eq. (20).

Calculations for rectangular distributions of pores provide a straightforward route to realistic results. The rectangular distribution of pore sizes is given respectively by $n(r) = n_0$ for $x_0 \le r \le x_m$ and zero for other values of r. The maximum value of r is taken to be the largest solute size ($r_m = x_m$) to avoid the effect of totally excluded solutes. The minimum value of r is chosen to ignore pores smaller than the smallest solute size, i.e., $r_0 = x_0$.

Calculations were also done with a gamma distribution of pore radii, for which the continuous variable r replaced x in Eq. (21). Log-normal or truncated Gaussian distributions, such as those used by Mochizuki and Zydney (1), could also be employed for $n(x)$.

FRACTAL PORE-SIZE DISTRIBUTIONS

Discrete pore-size distributions can be represented by a fractal power relation. A model of a porous membrane with a deterministic fractal distribution of pores is developed by a conceptual process of making parallel holes in a slab. A similar construction (14) was used for flow in a porous medium. Adler (14) suggested that such fractals could be applied to diffusion and conduction (thermal or electrical) but did not introduce mixtures of different sized molecules. The benefit of the fractal approach is that simple mathematical formulas describe the fractal properties. Adler's exposition (19) elaborates on the fractal representation of porous systems.

We first consider a membrane based on the fractal known as the Sierpinski carpet (13), and then generalize the concept to consider holes of different numbers, shapes, and sizes. Figure 2 shows the steps $j = 1, 2, 3$ in the construction of the membrane from a unit square of area a^2. At Step 1 a square hole of edge $a/3$ is formed perpendicular to the membrane. In each of the remaining 8 squares a hole of size $(a/3^2)^2$ is formed. This process is repeated indefinitely for every square. The edge length of a square at Step j is $r_j = a/3^j$ and its cross section has area $a^2/9^j$. The number and volume, respectively, of pores formed at the jth step are

$$n_j = 8^{j-1} \quad \text{and} \quad V_j = L(8/9)^j a^2/8 \tag{27}$$

Although not a fractal, the cumulative pore-volume distribution up to the jth step can be shown to be $La^2[1 - (8/9)^j]$, which becomes La^2 if $j \to \infty$, meaning that all mass is eventually removed by making square holes in the membrane. The discrete pore-volume distribution has the fractal property (13) that it can be represented by a noninteger power, or fractal dimension, D,

$$V_j = A^D r_j^{2-D} \tag{28}$$

where

$$D = \ln 8/\ln 3 \quad \text{and} \quad A = a(L/8)^{1/D} \tag{29}$$

The pore cross-section-area distribution is

$$V_j/L = A'^D r_j^{2-D} \tag{30}$$

where $D = \ln 8/\ln 3$ as before and $A' = a(1/8)^{1/D}$. The distribution can

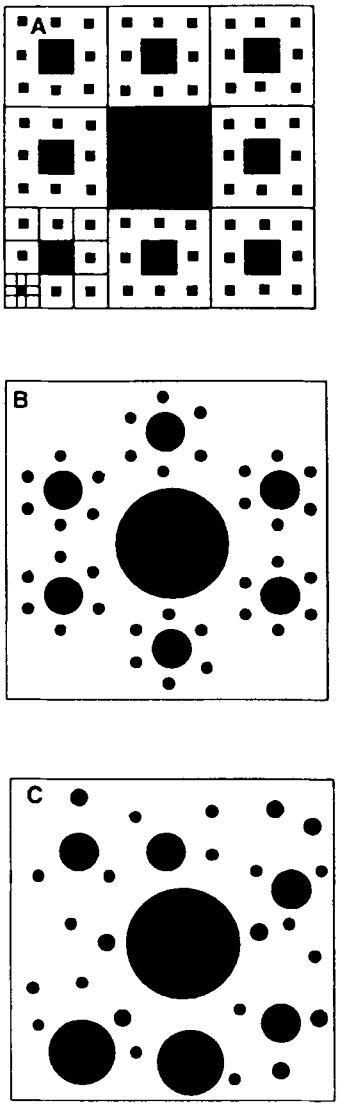

FIG. 2 Steps in the construction of fractal membranes: (A) Sierpinski membrane, i.e., $\Omega = 1$, $\sigma = 3$, $h = 8$, $j = 1$–3; (B) $\Omega = \pi$, $\sigma = 3$, $h = 6$, $j = 1$–3; (C) $\Omega = \pi$, $\sigma = 1.5$, $h = 2$, $j = 1$–5.

be made dimensionless:

$$V_j/La^2 = A^{*D}(r_j/a)^{2-D} \tag{31}$$

where D is unchanged and $A^* = 8^{-1/D}$

The fractal pore distribution can be generalized by considering pores of cross-sectional area Ωr_j^2, where $\Omega = 1$ for squares, π for circles, or other constants for other cross-section shapes. For membrane transport through parallel pores the placement of the pores is immaterial if the cross sections do not overlap and the upstream and downstream liquids are well-stirred. Even though the pores are positioned randomly over the membrane, the underlying fractal order of pore size applies. This melding of randomness and organization is a common property of porous systems (19). The relative size (e.g., radius) of the pores formed at two subsequent steps is defined as the constant σ:

$$\sigma = (\text{size of pore formed at Step } j)/(\text{size of pore formed at Step } j + 1) \tag{32}$$

The relative number of pores formed at subsequent steps is also a constant:

$$h = (\text{number of pores formed at Step } j + 1)/(\text{number of pores formed at Step } j) \tag{33}$$

A similar generalization of the Sierpinski carpet was suggested by Pfeifer and Obert (20). The unit square of area a^2 can be replicated side-by-side to form the total membrane surface area. The size of pores removed at Step j is $r_j = a/\sigma^j$, and the volume of a pore is $L\Omega(a/\sigma^j)^2$. The volume removed at the jth step is $L(\Omega a^2/h)/(h/\sigma^2)^j$, and the cumulative volume removed is $[L\Omega a^2/(\sigma^2 - h)][1 - (h/\sigma^2)^j]$. All the membrane mass is removed if the cumulative volume of pores at the jth step is La^2. Such a structure possesses fractal properties in a finite range of pore sizes. The fractal dimension D and the premultiplier A^* in the dimensionless equation

$$V_j/La^2 = A^{*D}(r_j/a)^{2-D} \tag{34}$$

can be shown to be

$$D = \ln h/\ln \sigma \quad \text{and} \quad A^* = (\Omega/h)^{1/D} \tag{35}$$

The fractal dimension D depends on σ and h but not on the shape factor Ω; the premultiplier A^* depends on h and Ω but not on σ. For the Sierpinski membrane (fractal over the entire range of pore sizes), $\Omega = 1$, $\sigma = 3$, and $h = 8$, and the expressions reduce appropriately. If $h = \sigma^2$, then the distribution is rectangular and discrete.

Examples of fractal constructions are pictured in Fig. 2. The Sierpinski carpet (A) shows the first three steps in making the square holes of size ratio $\sigma = 3$ and number ratio $h = 8$. A membrane with circular cross-section pores is shown (B) with $\sigma = 3$ and $h = 6$. The random positioning of the pores in the membrane (C) with $\sigma = 1.5$ and $h = 2$ does not affect the separation process.

Figure 3 shows the pore volume distribution versus r/a for various values of the parameters. The fractal membranes display pore-volume distributions that may either increase or decrease with pore size. One may utilize such power-law distributions as continuous distributions. For the discrete distribution, values of r_j are spaced evenly on the logarithmic axis by the amount $\log(\sigma)$. The line for the square-pore Sierpinski membrane would be parallel to the cylindrical-pore case for $\sigma = 3$ and $h = 8$ (not plotted). For a given value of σ, lines for different h intersect at $r = 1/\sigma$.

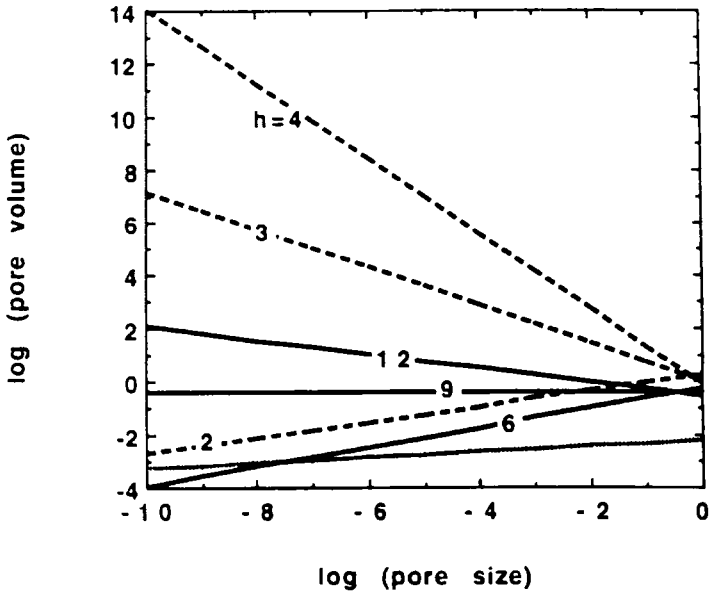

FIG. 3 Log-log plot of the pore-volume distribution: reduced volume, V_j/La^2, versus hole size, r_j/a, for fractal membranes with cylindrical holes ($\Omega = \pi$), $\sigma = 1.5$ (dashed line) and $\sigma = 3$ (solid line), and several values of h. The dotted line is the Sierpinski membrane ($\Omega = 1$, $\sigma = 3$, $h = 8$).

RESULTS AND DISCUSSION

It is instructive to view how the sieving coefficients $s(x)$ and S depend on the membrane and mixture parameters. In Fig. 4 are shown the solute sieving coefficients, $s(x)$, for several values of the transmembrane-pressure parameter, T_0, calculated by Eq. (25). This membrane has a rectangular pore-size distribution with $r_0/x_0 = 1$ and $r_m/x_0 = x_m/x_0 = 10$. The coefficient $s(x)$ is independent of the *distribution* of solute sizes. Calculations (not shown) for a gamma distribution of pore radii demonstrated behavior similar to Fig. 4. Solutes larger than $x/x_0 = 10$ are totally rejected ($s = 0$), while small solutes are readily transported by diffusion through the membrane if T_0 is small.

Figure 5 shows the same data as Fig. 4 but plotted as $s(x)$ versus T_0. If the Peclet number is large (e.g., T_0 is large), the sieving coefficient has its asymptotic value, $s_\infty(x) = \Phi K_c$. In the other limit, $P \ll 1$ (e.g., T_0 is small) and the solute transport is primarily diffusive, so that $s \approx 1$. The two limits are displayed in Fig. 5, where $s(x)$ is plotted for solutes of size $x/x_0 = 1, 2, 4, 6, 8$, and 10. Smaller solutes have higher values of $s(x)$ since they are more readily transported through the pores. The sieving

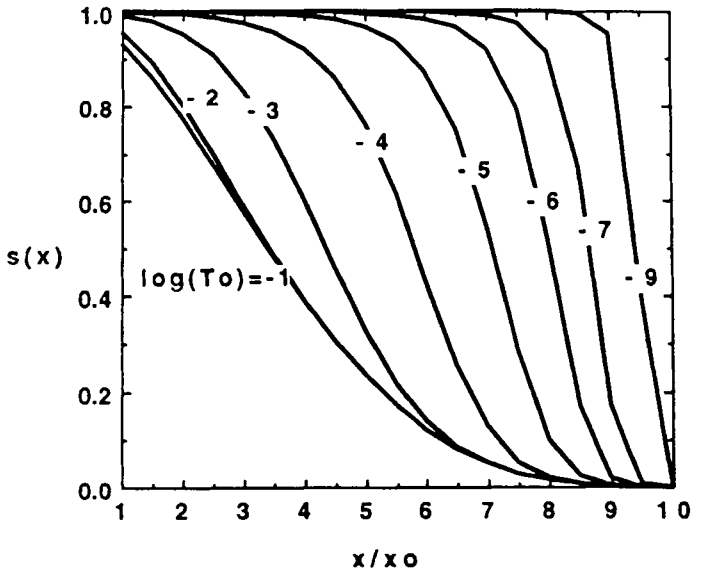

FIG. 4 The solute sieving coefficient, $s(x)$, for a gamma distribution of solutes and a rectangular distribution of pores ($x_m/x_0 = r_m/x_0 = 10$) for values of T_0 from 10^{-9} to 0.1.

coefficient $s(x)$ shows the same features as Fig. 5 of Mochizuki and Zydney (1), which also applies to distributed pores and solutes of distinct size.

The membrane sieving coefficient, S, calculated by Eq. (20), behaves in a similar manner if we plot S versus T_0 for given pore and solute distributions (Fig. 6). The computational results are for a gamma distribution of solutes and the rectangular distribution of pores used in Figs. 4 and 5. As the solute distribution broadens, i.e., β increases, the large T_0 asymptote decreases due to hindered transport of the larger solutes in the broadened distribution. For small T_0 the membrane sieving coefficient S approaches unity since the maximum size of solutes equals the maximum size of pores ($r_m/x_0 = x_m/x_0 = 10$). In this limit S would be less than unity if $r_m < x_m$, i.e., the feed solution has solutes larger than the membrane cutoff. Thus, as commonly defined, the *membrane* cutoff excludes solutes larger than the largest pore.

The results for discrete pore distributions demonstrate behavior similar to that of the continuous distributions. The solute sieving coefficient $s(x)$ is calculated by Eq. (15) and plotted for several values of T_0 in Fig. 7 for a fractal distribution of pores with $s = 1.5$, $h = 2$, $a/x_0 = 10$ (values of

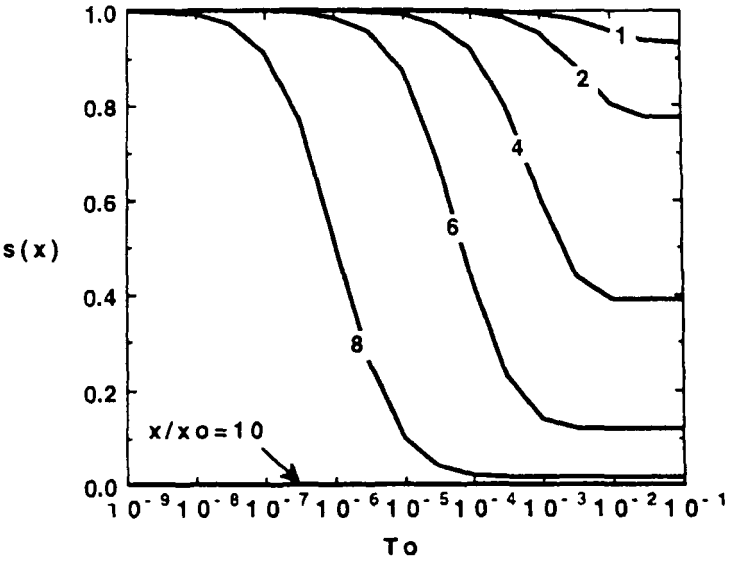

FIG. 5 The solute sieving coefficient, $s(x)$, versus the parameter for transmembrane pressure, T_0 (same conditions as Fig. 4). As solute size increases, the diffusive asymptote decreases.

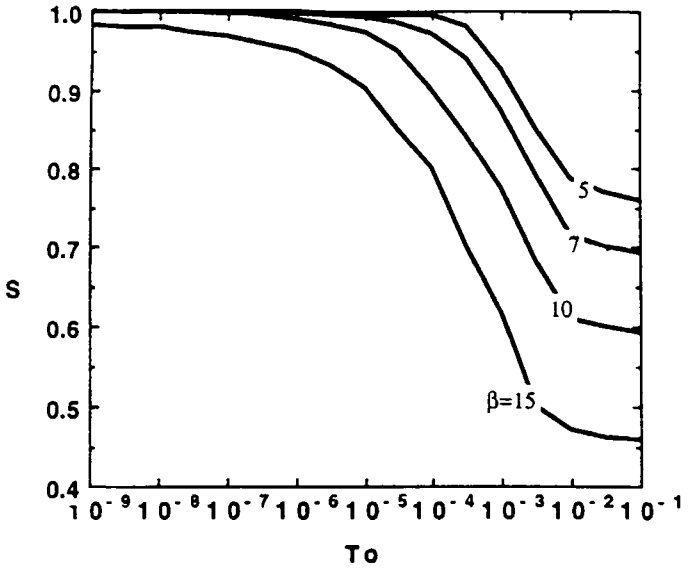

FIG. 6 The membrane sieving coefficient, S, for a gamma distribution of solutes and a rectangular distribution of pore sizes. As the solute distribution broadens (β increases), the diffusive asymptote decreases.

r_j and V_j are given in Table 1). This plot shows that as T_0 decreases, diffusive transport allows solute concentrations to be more nearly equal on the two sides of the membrane, and $s(x)$ approaches unity for a larger range of pore sizes. Figure 8 is the same as Fig. 7 but with $h = 40$. As the relatively larger numbers of small pores restricts the permeation of larger solutes, all curves for given values of T_0 are shifted leftward to smaller values of x/x_0.

The relationship between $c_0(x)$ and $c_f(x)$ is shown in Fig. 1 for the fractal distribution of pores ($h = 2$) and for two values of β (width of solute distribution). The sieving action of the membrane serves to reduce the size of the filtrate solutes, i.e., $c_f \leq c_0$ for all x.

The effect on the membrane sieving coefficient of changing h is demonstrated in Fig. 9, where S calculated by Eq. (20) is plotted versus T_0. Computed values are displayed for $h = 2, 5, 10, 40$, and 100. As the pore-size distribution shifts to smaller sizes (i.e., as h increases), S decreases. The effect on the diffusive asymptote (large T_0 value of S) is especially strong.

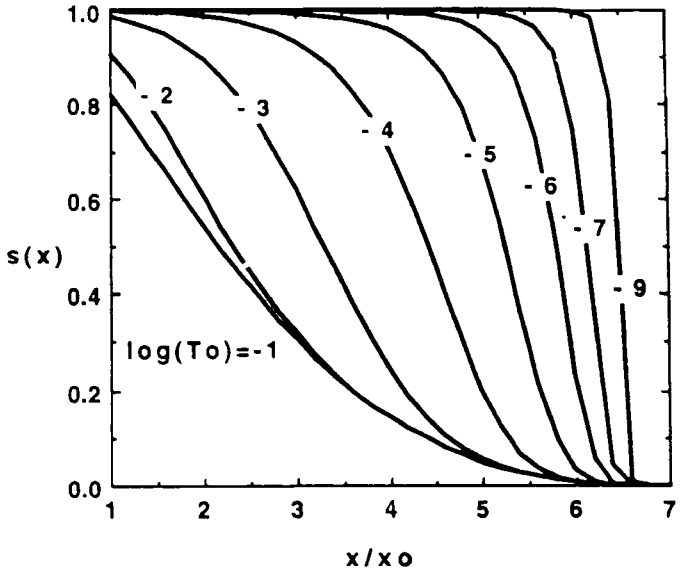

FIG. 7 The solute sieving coefficient, $s(x)$, for a gamma distribution of solutes (x_m/x_0 = 7) and a fractal distribution of pores (h = 2, σ = 1.5, Ω = π, a/x_0 = 10) for values of T_0 from 10^{-9} to 0.1.

The results clearly demonstrate that sieving coefficients are influenced by both the pore-size and solute-size distributions. Not only cutoff properties, but also hindered transport enters into the analysis of ultrafiltration separations. Using an average pore size for computations and data analysis will not in general suffice to reveal the true behavior of a polydisperse-mixture membrane separation process.

TABLE 1
Pore Size and Pore Volume for Six Steps in the Construction of a Fractal Distribution of Pores (σ = 1.5, Ω = π, a = $10x_0$)

		V_j/La^2		
j	r_j/a	h = 2	h = 3	h = 5
1	0.6667	1.158	1.356	1.977
2	0.4444	1.029	1.808	4.393
3	0.2963	0.915	2.411	9.762
4	0.1975	0.813	3.215	21.69
5	0.1317	0.723	4.286	48.21
6	0.0978	0.622	5.715	107.1

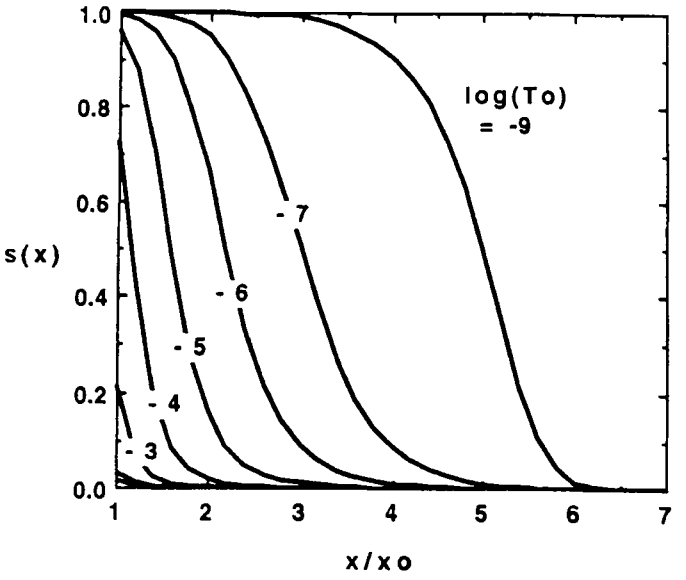

FIG. 8 The solute sieving coefficient for conditions of Fig. 6 except that $h = 40$.

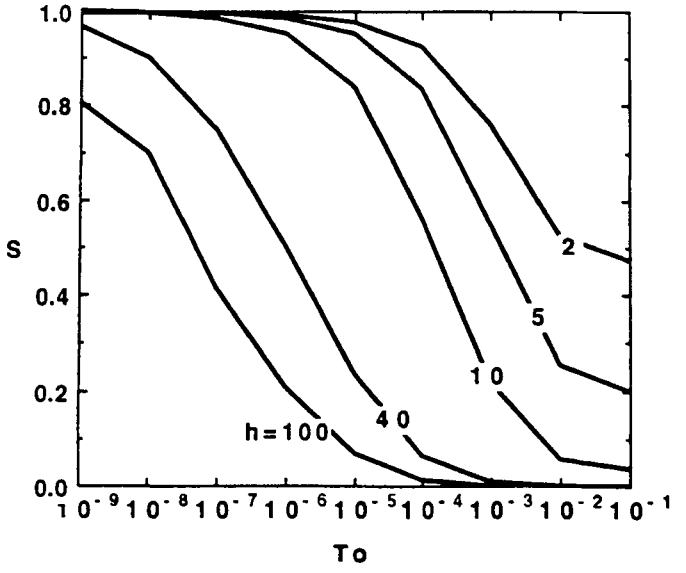

FIG. 9 The membrane sieving coefficient, S, versus T_0 for a fractal membrane with $\sigma = 1.5$ and $\Omega = \pi$. The pore distribution shifts to smaller sizes as h increases.

CONCLUDING REMARKS

Combining distributed pore and solute sizes in membrane separation theory deepens the understanding of ultrafiltration processes. The interaction of pores and solutes of different sizes gives rise to behavior not readily interpreted by simpler models. The present work provides a framework for developing more detailed theories that may be useful in designing membrane processes and explaining experimental observations.

The present approach to membrane sieving differs from other models by explicitly accounting for the distribution of solute sizes as well as of pore sizes. The continuous-mixture concept of polydispersivity allows a hydrodynamic analysis of hindered pore transport that leads to the computation of sieving coefficients. The sieving coefficient for individual solutes, $s(x)$, is useful for calculating the downstream (filtrate) solute-size distribution, $c_f(x)$, given the upstream distribution, $c_0(x)$. An integration computation allows the membrane sieving coefficient, S, to be calculated from $s(x)$ and $c_0(x)$. The theory reduces appropriately to simpler models; for example, discrete solute mixtures in distributed pores and monodisperse solutes in monodisperse pores. The distribution functions, gamma distributions for solutes, and continuous rectangular and discrete fractal distributions for pores are easily replaced in the model with other functions. Characterization of the mixtures by gel permeation chromatography and direct measurement of the membrane pore-size distribution by electron microscopy can furnish the essential information needed to implement the theory and test it against experimental observations.

The current model is limited by several approximations and assumptions. The membrane concentration polarization and fouling are neglected, even though the polydisperse solute distribution affects this phenomena (12). We consider the diffusion coefficient to be invariant with solute size, a satisfactory approximation for narrow distributions. All pores are perpendicular to the membrane and therefore of the same length. The calculations for hindered transport apply to very dilute solutions of rigid spherical solutes in cylindrical pores with none but steric pore-wall interactions (e.g., no adsorption or electrostatic activity). In all except the most dilute mixtures, however, solutes in pores will obstruct the permeation of other solutes (21). While some of these approximations can be mitigated, relaxation of the assumptions inherent in the hydrodynamic theory of hindered pore transport must await advances in this fundamental issue of fluid dynamics. Some of the basic ideas outlined in the current approach, however, will possibly be unchanged.

NOMENCLATURE

a_n, b_n coefficients in expressions for hindered transport quantities K_t and K_s (n = 1–7):

$a_1 = -73/60$
$a_2 = 77{,}293/50{,}400$
$a_3 = -22.5083$
$a_4 = -5.6117$
$a_5 = -0.3363$
$a_6 = -1.216$
$a_7 = 1.647$
$b_1 = 7/60$
$b_2 = -2227/50{,}400$
$b_3 = 4.018$
$b_4 = -3.9788$
$b_5 = -1.9215$
$b_6 = 4.392$
$b_7 = 5.006$

a	length scale for a membrane of unit surface area a^2
A, A', A^*	coefficients in fractal expressions for membrane pore volume V_j
$c(x)$	distribution of solutes of radii x
$c_0(x)$	upstream distribution of solutes of radii x
$c_f(x)$	downstream (filtrate) distribution of solutes of radii x
C	lumped concentration; integral of $c(x)$ over all x
C_0	concentration of upstream solutes
C_f	concentration of downstream solutes
D	fractal dimension for membrane pore volume V_j
D_b	bulk-solution diffusivity
$J(x, r)$	flux of solute of radius x through pore of radius r
K_c, K_d, K_s, K_t	hindrance factors for solute transport in a pore
L	thickness of membrane
$n(r)$	distribution of pores of radius r
n_j	number of pores of radius r_j
$N(x)$	permeation rate of solute of radius x
P_j	Peclet number for transport in a pore of radius r_j
Δp	transmembrane pressure difference
Q	total volumetric flow rate through membrane
r	radius of a pore for continuous pore-size distributions

r_j	discrete values of pore radius ($j = 1, 2, 3, \ldots$)
r_0	minimum pore radius in a membrane
r_m	maximum pore radius in a membrane
S	membrane sieving coefficient in terms of lumped concentrations
$s(x)$	membrane sieving coefficient for solute of radius x
T_0	dimensionless parameter, e.g., for transmembrane pressure
v_j	cross-section average velocity in a pore of radius r_j
V_j	volume of pores of size r_j
x	solute radius
x_0	minimum solute radius in a distribution
x_m	maximum solute radius in a distribution
z	length coordinate along the pore
α	parameter in the gamma distribution
β	parameter in the gamma distribution
Φ	partition function
μ	viscosity of solvent
σ	parameter in fractal distribution of pore sizes
$\Gamma(\alpha)$	gamma function [$= (\alpha - 1)!$ if α is an integer]
Ω	shape factor for pores

REFERENCES

1. S. Mochizuki and A. L. Zydney, "Theoretical Analysis of Pore Size Distribution Effects on Membrane Transport," *J. Membr. Sci.*, *82*, 211 (1993).
2. S. Mochizuki and A. L. Zydney, "Dextran Transport through Asymmetric Ultrafiltration Membranes: Comparison with Hydrodynamic Models," *Ibid.*, *68*, 21 (1992).
3. W. S. Opong and A. L. Zydney, "Diffusive and Convective Protein Transport through Asymmetric Membranes," *AIChE J.*, *37*, 1497 (1991).
4. L. Zeman and M. Wales, "Polymer Solute Rejection by Ultrafiltration Membranes," in *Synthetic Membranes, Vol. II, ACS Symp. Ser.*, *154* 411–434 (1981).
5. W. M. Deen, "Hindered Transport of Large Molecules in Liquid-Filled Pores," *AIChE J.*, *33*, 1409 (1987).
6. P. M. Bungay and H. Brenner, "The Motion of a Closely Fitting Sphere in a Fluid Filled Tube," *Int. J. Multiphase Flow*, *1*, 25 (1973).
7. G. Astarita and S. I. Sandler (Eds.), *Kinetic and Thermodynamic Lumping of Multicomponent Mixtures*, Elsevier, 1991.
8. A. V. Sapre and F. J. Krambeck (Eds.), *Chemical Reactions in Complex Mixtures*, Van Nostrand Reinhold, 1991.
9. R. Aris, "On Almost Discrete Γ-Distributed Chemical Species and Reactions," *Chem. Eng. Sci.*, *49*, 581 (1994).
10. M. Wang, C. Zhang, J. M. Smith and B. J. McCoy, "Continuous-Mixture Kinetics of Thermolytic Extraction of Coal in Supercritical Fluid," *AIChE J.*, *40*, 131 (1994).
11. B. J. McCoy, "Continuous-Mixture Kinetics and Equilibrium for Reversible Oligomer-

ization Reactions," *Ibid.*, *39*, 1827 (1993).
12. H. B. Dharmappa, J. Verink, R. Ben Aim, K. Yamamoto, and S. Vigneswaran, "A Comprehensive Model for Cross-Flow Filtration Incorporating Polydispersity of the Influent," *J. Membr. Sci.*, *65*, 173 (1992).
13. B. B. Mandelbrot, *The Fractal Geometry of Nature*, W. H. Freeman and Co., 1977.
14. P. M. Adler, "Flow in Porous Media," in D. Avnir (Ed.), *The Fractal Approach to Heterogenous Chemistry*, Wiley, New York, 1989, p. 341.
15. M. Sernetz, H. R. Bittner, H. Willems, and C. Baumhoer, "Chromatography," in D. Avnir (Ed.), *The Fractal Approach to Heterogeneous Chemistry*, Wiley, 1989, p. 361.
16. J. C. Giddings, E. Kucera, C. P. Russell, and M. N. Myers, "Statistical Theory for the Equilibrium Distribution of Rigid Molecules in Inert Porous Networks: Exclusion Chromatography," *J. Phys. Chem.*, *72*, 4397 (1968).
17. J. C. Giddings, *Unified Separation Science*, Wiley-Interscience, New York, 1991, pp. 31–35.
18. M. Abramowitz and I. A. Stegun, *Handbook of Mathematical Functions*, National Bureau of Standards, 1968, Chap. 26.
19. P. M. Adler, *Porous Media—Geometry and Transports*, Butterworth-Heinemann, Boston, 1992.
20. P. Pfeifer and M. Obert, "Fractals: Basic Concepts and Terminology," in D. Avnir (Ed.), *The Fractal Approach to Heterogeneous Chemistry*, Wiley, New York, 1989, p. 35.
21. C. M. Tam and A. Y. Tremblay, "Membrane Pore Characterization—Comparison between Single and Multicomponent Solute Probe Techniques," *J. Membr. Sci.*, *57*, 271 (1991).

Received by editor June 22, 1994